

Self-assembly of quantum dots: effect of neighbor islands on the wetting in coherent Stranski-Krastanov growth

José Emilio Prieto*

Institut für Experimentalphysik, Freie Universität Berlin, Arnimallee 14, 14195 Berlin, Germany

Ivan Markov†

Institute of Physical Chemistry, Bulgarian Academy of Sciences, 1113 Sofia, Bulgaria

(Dated: November 18, 2018)

The wetting of the homogeneously strained wetting layer by dislocation-free three-dimensional islands belonging to an array has been studied. The array has been simulated as a chain of islands in 1+1 dimensions. It is found that the wetting depends on the density of the array, the size distribution and the shape of the neighbor islands. Implications for the self-assembly of quantum dots grown in the coherent Stranski-Krastanov mode are discussed.

PACS numbers: 68.35.Md, 68.35.Np, 68.65.Hb, 68.43.Hn

The instability of planar films against the development of coherently strained three-dimensional (3D) islands in highly mismatched epitaxy is a subject of intense research in recent times due to the optoelectronic applications of the islands as quantum dots.¹ The term “coherent Stranski-Krastanov (SK) growth” has been coined for this formation of 3D islands that are strained to fit the underlying wetting layer but are nearly strainfree near their top and side walls,^{2,3} in contrast to the “classical” SK growth in which the lattice mismatch is accommodated by misfit dislocations at the interface with the wetting layer.⁴

Experimental studies of arrays of coherent 3D islands of semiconductor materials have shown surprisingly narrow size distributions.^{5,6,7,8} This phenomenon, known as self-assembly,⁹ is highly desirable as it guarantees a specific optical wavelength of the array of quantum dots. The physics of the self-assembly is still not well understood in spite of several studies.^{10,11,12,13} Priester and Lannoo found that two-dimensional (2D) monolayer-high islands have a minimal energy per atom for a certain size and act as precursors of the 3D pyramidal islands, which become energetically favored at a smaller volume.¹⁴ Thus at some critical surface coverage the 2D islands spontaneously transform into 3D ones preserving a nearly constant volume. The resulting size distribution reflects that of the 2D islands which is very narrow. This picture has been recently corroborated by Ebiko *et al.*¹⁵ who found that the volume distribution of InAs/GaAs self-assembled quantum dots agrees well with the scaling function characteristic of submonolayer homoepitaxy.¹⁶ Korutcheva *et al.*¹⁷ and Markov and Prieto¹⁸ reached the same conclusion with the exception that the 2D-3D transformation was found to take place through a series of intermediate states with discretely increasing thickness, in monolayer (ML) steps, that are stable in separate consecutive intervals of volume. Khor and Das Sarma arrived to the same conclusion using Montecarlo simulations.¹⁹

The formation of coherent 3D islands has been discussed within the framework of the traditional concept of wetting.²⁰ The wetting parameter, which accounts for the

energetic influence of a crystal B in the heteroepitaxy of a crystal A on top of it, is defined as²¹ $\Phi = 1 - E_{AB}/E_{AA}$, where E_{AA} and E_{AB} are the energies per atom required to disjoin a half-crystal A from a like half-crystal A and from an unlike half-crystal B, respectively. The mode of growth of a thin film is determined by the difference $\Delta\mu = \mu(n) - \mu_{3D}^0$, where $\mu(n)$ and μ_{3D}^0 are the chemical potentials of the film (as a function of its thickness n) and of the bulk material A, respectively.²¹ The chemical potential of the bulk crystal A is given at zero temperature by $-\phi_{AA}$, the negative of the binding energy of an atom to the well known kink or half-crystal position. At this position the atom is bound to a half-atomic row, a half-crystal plane and a half-crystal block.²² In the case of a monolayer-thick film of A on the surface of B the chemical potential of A is given by the analogous energy $-\phi_{AB}$ when the underlying half-crystal block of A is replaced by a half-crystal block of B. Thus $\Delta\mu = \phi_{AA} - \phi_{AB}$. In the simplest case of additivity of bond energies this difference reduces to $E_{AA} - E_{AB}$. Then $\Delta\mu$ is proportional to Φ , i.e. $\Delta\mu = E_{AA}\Phi$.²¹ It follows that the wetting parameter Φ determines in fact the mechanism of growth of A on B.²³

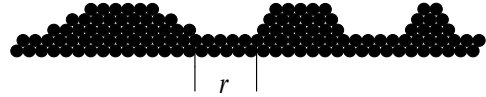


FIG. 1: Schematic view of an array of islands on a wetting layer. The central island is surrounded by two islands with different shapes and sizes. The spacing between neighbor islands is denoted by r , which is a measure of the density of the array.

In the present work we study the behavior of Φ for islands that belong to an array. For the coherent SK growth, which is in fact the formation of dislocation-free 3D islands of A on the same (strained) material A, it is convenient to define the wetting parameter Φ as the difference of the interaction energies of misfitting and non-misfitting 3D islands with the wetting layer.²⁰ We study

the effect of the array density and of the size and shape distributions of neighbor islands on the wetting parameter Φ of a given island. We consider an atomistic model in 1 + 1 dimensions which can be regarded as a cross-section of the real 2 + 1 case. An implicit assumption is that the islands have a compact rather than a fractal shape and that the lattice misfit is the same in both orthogonal directions. The 3D islands are represented by linear chains of atoms stacked one upon the other.²⁴ The shape of the islands in our model is given by the slope of the side walls. The array in the 1+1 dimensional space is represented by a row of 3 or 5 islands on a wetting layer consisting of several monolayers (Fig. 1). The distance between two neighbor islands is given by the number r of vacant atomic positions between the ends of their base chains.

In order to simplify the computational procedure, the “wetting layer” in our model is in fact composed of several monolayers of the true wetting layer of the overlayer material A plus several monolayers of the unlike substrate material B. This composite wetting layer has the atom spacing of the substrate material B as is the real case, but for the sake of simplicity, it has the atom bonding of the overlayer material A. This underestimates somewhat the value of Φ because the A-A bonding is weaker than the B-B bonding, but it does not introduce a significant error as the energetic influence of the substrate B is screened by the true wetting layer A.

To find the equilibrium atomic positions, we make use of a simple minimization procedure.¹⁸ The atoms interact through a Morse potential $V(x) = V_0 [e^{-12(x-a)} - 2e^{-6(x-a)}]$. We calculate the interaction energy of all the atoms as well as its gradient with respect to the atomic coordinates, i.e. the forces. Relaxation of the system is performed by allowing the atoms to displace in the direction of the gradient in an iterative procedure until the forces fall below some negligible cutoff value. Periodic boundary conditions are applied in the lateral direction. We consider only interactions with first neighbors.

As expected, the edge atoms are found to be more weakly bound to the underlying wetting layer than the center atoms (Fig. 2). Compared to an isolated island, the edge atoms of an island in an array adhere weaker to the substrate. This is in fact the essential physical effect exerted by the neighbors on a given island: it loses contact with the substrate and the wetting parameter is increased. We can regard this as the substrate becoming stiffer under the influence of the neighbor islands.

The influence of the density of the array is demonstrated in Fig. 3. As expected, the wetting parameter increases with increasing array density. The figure also allows us to estimate the size of the effect. At a distance $r=10$ (about 30 nm), neighbors make Φ increase by 10%; this represents an effective decrease in adhesion ΔE_{AB} of $0.10 \Phi E_{AA}$. For Ge/Si(100) (desorption energy of Ge: 4 eV), this gives about 20 meV, a contribution of the same order as the elastic energy per atom (40 meV in this system²¹) that can significantly affect the delicate

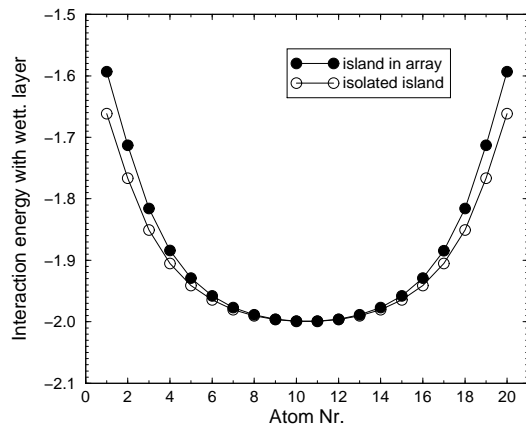


FIG. 2: Distribution of the energy (in units of V_0) between the atoms of the base chain of a 3 ML-high, coherent island of 20 atoms in the base chain, and the underlying wetting layer, for a positive misfit of 8%. Full circles correspond to an island separated by a distance $r = 5$ from two identical neighbors, while the empty ones correspond to a reference isolated island.

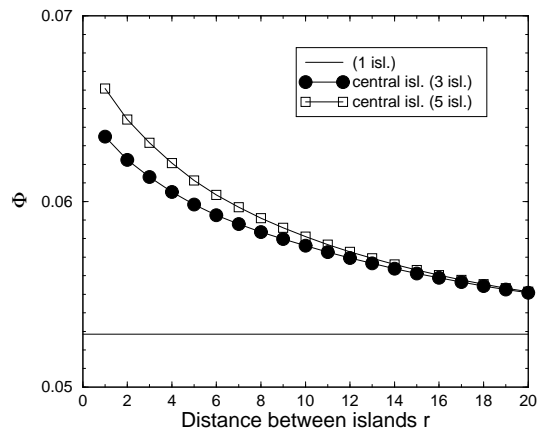


FIG. 3: Dependence of the wetting parameter of the central island on the distance r between the islands. All islands are 3 ML high and have 20 atoms in the base chain. The lattice misfit amounts to 7%. Results for arrays of 3 and 5 islands are given, as well as for a reference isolated island.

balance of the energies involved in the growth process: diffusion barriers and surface/interface energies.

Figure 4 shows the wetting parameter of the central island vs. the size of the side islands. Increasing the volume of the side islands leads to an increase of the elastic fields around them and to a further reduction of the bonding between the edge atoms of the central island and the wetting layer.

Figure 5 demonstrates one further important result, the effect of the size distribution on the wetting of the islands. It shows the behavior of the wetting parameter Φ of the central island as a function of the number of atoms in the base chain of the left island. The sum of the total number of atoms of left and right islands is

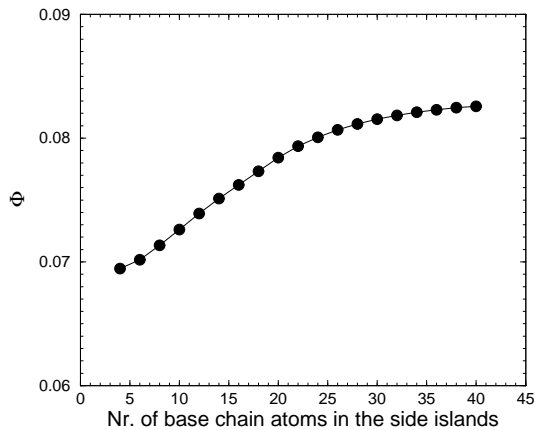


FIG. 4: Dependence of the wetting parameter of the central island on the size of the two side islands. These two have equal volumes and are separated from the central one by a distance $r = 5$. All the islands are 3 ML high, the central one has 20 atoms in the base chain and the misfit amounts to 7%.

kept constant and precisely equal to the doubled number of the central island. The facet angle of all three islands is 60° . Thus the first (and the last) points give the maximum asymmetry in the size distribution of the array, the left (right) island containing 9 atoms and the right (left) island 105. All three islands are 3 ML thick. The point at the maximal wetting corresponds to the monodisperse distribution: the three islands having one and the same volume of 57 atoms. This means that in the case of perfect self-assembly of the array, the wetting parameter and therefore the tendency to clustering display a maximum value.

The effect of the shape of the side islands, i.e. their facet angles, on the wetting parameter of the central island is demonstrated in Fig. 6. The facet angle of the central island is 60° . The effect is greatest when the side islands have the steepest walls. The same result (not shown) is obtained when the central island has a different shape. The explanation follows the same line as the one given above: islands with larger-angle side walls exert a greater elastic effect on the substrate and in turn on the displacements and the bonding of the edge atoms of the central island.

When discussing the above results we have to bear in mind that a positive value of the wetting parameter implies in fact a tendency of the deposit to form 3D clusters instead of a planar film. In the case of coherent SK growth the non-zero wetting parameter is due to the weaker adhesion of the atoms close to the island's edges. The presence of other islands, particularly with large angle facets, in the near vicinity enhances the effect. The transformation of 2D, monolayer-high islands into bilayer islands takes place by detachment of atoms from the edges and their subsequent jumping and nucleating on the top island's surface.²⁵ This edge effect hints at the influence of the lattice misfit on the rate of sec-

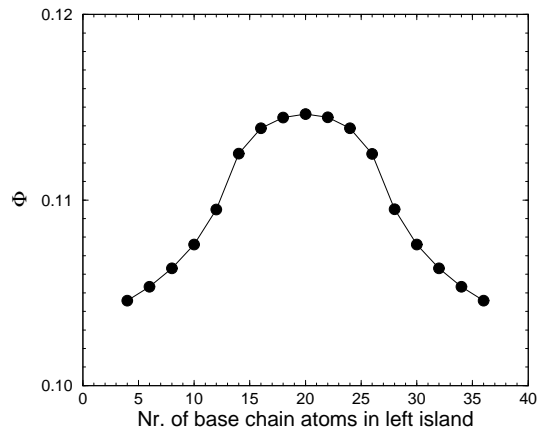


FIG. 5: Dependence of the wetting parameter of the central island on the size distribution of the side islands. The islands are 3 ML thick and are separated by a distance $r = 5$; the central one has 20 atoms in the base chain. The misfit amounts to 8%. The sum of the volumes of left and right islands is kept constant and equal to the doubled volume of the central island. At the center, the three islands have equal volumes.

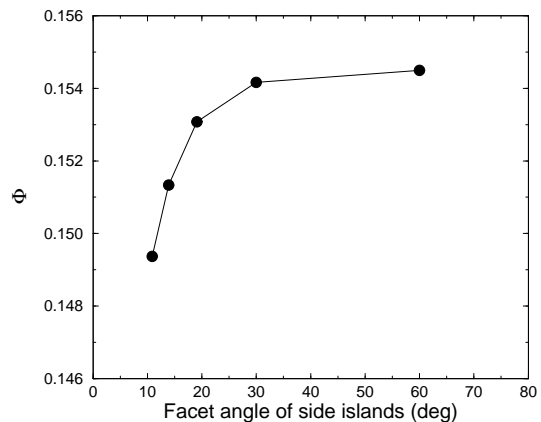


FIG. 6: Dependence of the wetting parameter of the central island on the shape of the neighbor islands, as given by the facet angle of their side walls. The central island has side walls of 60° . All islands are 3 ML high, have 20 atoms in their base chains and are separated by a distance $r = 5$. The misfit amounts to 8%.

ond layer nucleation and in turn on the kinetics of the 2D-3D transformation.^{26,27} The presence of neighbor islands favors the formation of 3D clusters and their further growth. For the self-assembled monodisperse population, the highest tendency to clustering is found.

We can regard the flatter islands in our model (11° facet angle) as the “hut” clusters discovered by Mo *et al.*,²⁸ and the clusters with 60° facet angle as the “dome” clusters. It is well known that clusters with steeper side walls relieve the strain more efficiently than flatter clusters²⁹ (a planar film, the limiting case of the flat islands, does not relieve strain at all). We see that large-angle facet islands affect more strongly the growth of the neigh-

bor islands, leading to a more narrow size distribution.

From our results, a self-assembled population of quantum dots with highest density is expected at comparatively low temperatures such that the critical wetting layer thickness for 3D islanding approaches an integer number of monolayers. In InAs/GaAs quantum dots the reported values of the critical thickness are found to vary from 1.2 to 2 ML.³⁰ The critical wetting layer thickness is given by an integer number n of monolayers plus the product of the 2D island density and the critical volume N_{12} in the $(n+1)$ -th ML. The 2D island density increases steeply with decreasing temperature.¹² In such a case a dense population of 2D islands will overcome simultaneously the critical size N_{12} to produce bilayer islands. The value of N_{12} will be slightly reduced when neighbor islands are present due to the increase of Φ .²⁰ Regions of high adatom concentrations will favor the highest degree of self-assembly and, due to the larger elastic forces present, are also likely to promote the spatial ordering of the islands, possibly extending to less dense regions and leading to self-organized arrays. Islands will thus interact with each other from the very beginning of the 2D-3D transformation and will give rise to the maximum possible wetting parameter and, in turn, to islands with large-angle facets and a narrow size distribution. This

is in agreement with the observations of self-assembled Ge quantum dots on Si(001).³¹ At 700°C a population of islands with a concentration ranging from 10^7 to 10^8 cm^{-2} is obtained. The islands have the shape of truncated square pyramids with their side wall facets formed by (105) planes (inclination angle of about 11°). The size distribution of the islands is quite broad. At 550°C a population of islands with an areal density of the order of 10^9 to 10^{10} cm^{-2} is observed. The islands have larger-angle (113) facets and their size distribution is much more narrow.

In summary, the presence of neighbor islands decreases the wetting of the substrate (in this case the wetting layer) by the 3D islands. The wetting decreases with increasing array density and facet angle of the neighbor islands. The wetting parameter displays a maximum (implying a minimal wetting) when the array shows a monodisperse size distribution. We expect an optimum self-assembled islanding at low temperatures such that the 2D-3D transformation takes place at the highest possible island density.

J. E. P. gratefully acknowledges financial support from the Alexander-von-Humboldt Stiftung and the Spanish MEC (grant No. EX2001 11808094).

* Electronic address: jeprieto@physik.fu-berlin.de

† Electronic address: imarkov@ipchp.ipc.bas.bg

¹ P. Politi, G. Grenet, A. Marty, A. Ponchet, and J. Villain, Phys. Rep. **324**, 271 (2000).

² D. J. Eaglesham and M. Cerullo, Phys. Rev. Lett. **64**, 1943 (1990).

³ V. A. Shchukin and D. Bimberg, Rev. Mod. Phys. **71**, 1125 (1999).

⁴ J. W. Matthews, D. C. Jackson and A. Chambers, Thin Solid Films **29**, 129 (1975).

⁵ D. Leonard, M. Krishnamurthy, C. M. Reaves, S. P. Denbaars, and P. M. Petroff, Appl. Phys. Lett. **63**, 3203 (1993).

⁶ J. M. Moison, F. Houzay, F. Barthe, L. Leprince, E. André, and O. Vatel, Appl. Phys. Lett. **64**, 196 (1994).

⁷ M. Grundmann *et al.* Phys. Rev. Lett. **74**, 4043 (1995).

⁸ Z. Jiang, H. Zhu, F. Lu, J. Qin, D. Huang, X. Wang, C. Hu, Y. Chen, Z. Zhu, and T. Yao, Thin Solid Films **321**, 60 (1998).

⁹ C. Teichert, Phys. Rep. **365**, 335 (2002).

¹⁰ J. Tersoff and R. M. Tromp, Phys. Rev. Lett. **70**, 2782 (1993); J. Tersoff and F. K. LeGoues, Phys. Rev. Lett. **72**, 3570 (1994).

¹¹ V. A. Shchukin, N. N. Ledentsov, P. S. Kop'ev, and D. Bimberg, Phys. Rev. Lett. **75**, 2968 (1995).

¹² B. A. Joyce, J. L. Sudijono, J. G. Belk, H. Yamaguchi, X. M. Zhang, H. T. Dobbs, A. Zangwill, D. D. Vvedensky, and T. S. Jones, Jpn. J. Appl. Phys., Part 1 **36**, 4111 (1997).

¹³ H. M. Koduvally and A. Zangwill, Phys. Rev. B **60**, R2204 (1999).

¹⁴ C. Priester and M. Lannoo, Phys. Rev. Lett. **75**, 93 (1995).

¹⁵ Y. Ebiko, S. Muto, D. Suzuki, S. Itoh, H. Yamakoshi, K.

Shiramine, T. Haga, K. Unno, and M. Ikeda, Phys. Rev. B **60**, 8234 (1999).

¹⁶ J. G. Amar and F. Family, Phys. Rev. Lett. **74**, 2066 (1995).

¹⁷ E. Korutcheva, A. M. Turiel and I. Markov, Phys. Rev. B **61**, 16890 (2000).

¹⁸ I. Markov and J. E. Prieto, NATO ASI Series *Atomistic aspects of Epitaxial Growth*, vol.65, eds. M. Kotrla, N. Papanicolaou, D. D. Vvedensky and L. T. Wille, (Kluwer, 2002), p. 411.

¹⁹ K. E. Khor and S. Das Sarma, Phys. Rev. B **62**, 16657 (2000).

²⁰ J. E. Prieto and I. Markov, Phys. Rev. B **66**, 073408 (2002).

²¹ I. Markov, *Crystal Growth for Beginners*, 2nd edition, (World Scientific, 2003).

²² I. N. Stranski, Z. Phys. Chem. (Leipzig) **136**, 259 (1928).

²³ R. Peierls, Phys. Rev. B **18**, 2013 (1978).

²⁴ C. Ratsch and A. Zangwill, Surf. Sci. **293**, 123 (1993).

²⁵ S. Stoyanov and I. Markov, Surf. Sci. **116**, 313 (1982).

²⁶ S. N. Filimonov and Yu. Yu. Hervieu, Surf. Sci. **507-510**, 270 (2002).

²⁷ C. H. Lin and Y.-C. Tsai, Surf. Sci. **512**, 287 (2002).

²⁸ Y.-W. Mo, D. E. Savage, B. S. Swartzentruber, and M. Lagally, Phys. Rev. Lett. **65**, 1020 (1990).

²⁹ M. Horn-von Hoegen, Surf. Sci. **537**, 1 (2003).

³⁰ A. Polimeni, A. Patané, M. Capizzi, F. Martelli, L. Nasi, and G. Salviati, Phys. Rev. B **53**, R4213 (1996).

³¹ V. Le Tanh, P. Boucaud, D. Débarre, Y. Zheng, D. Bouchier, and J.-M. Lourtioz, Phys. Rev. B **58**, 13115 (1998).